Heliyon 10 (2024) e26337

Contents lists available at ScienceDirect

Heliyon

journal homepage: www.cell.com/heliyon

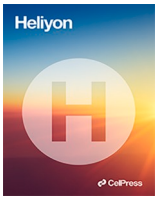

Research article

Design and performances improvement of an UWB antenna with DGS structure using a grey wolf optimization algorithm

Islem Bouchachi [a], Abdelmalek Reddaf [b], Mounir Boudjerda [b], Khaled Alhassoon [c,*], Badreddine Babes [b], Fahad N. Alsunaydih [c], Enas Ali [d], Mohammad Alsharef [e], Fahd Alsaleem [c]

[a] *Ecole Nationale Supérieure des Technologies Avancées, Algiers, Algeria*
[b] *Research Center in Industrial Technologies CRTI, B.P. 64, Cheraga, Algiers, Algeria*
[c] *Department of Electrical Engineering, College of Engineering, Qassim University, Buraydah 52571, Saudi Arabia*
[d] *Centre of Research Impact and Outcome, Chitkara University Institute of Engineering and Technology, Chitkara University, Rajpura, 140401, Punjab, India*
[e] *Department of Electrical Engineering, College of Engineering, Taif University, P. O. Box 11099, Taif, 21944, Saudi Arabia*

ARTICLE INFO

Keywords:
GWO algorithm
SWB antenna
DGS
SRR
CSSR
IoT

ABSTRACT

In this article, we propose the design of a rectangular-shaped patch antenna suitable for ultra-wideband (UWB) applications and short and long–range Millimeter-Wave Communications. We begin with the design of a high-gain UWB rectangular patch antenna featuring a partial ground plane and operating within the 3.1–10.6 GHz bandwidth. Complementary Split Ring Resonators (CSRRs) are integrated on both sides of the structure to meet desired specifications. The resulting UWB antenna boasts an extended frequency bandwidth, covering 2.38–22.5 GHz (twice that of the original antenna), with a peak gain of 6.5 dBi and an 88% radiation efficiency. The grey wolf optimization technique (GWO) determines optimal structural dimensions. Validation of the antenna's performance is demonstrated through the strong agreement between measurement and simulation.

1. Introduction

Ultra-Wideband (UWB) technology has a wide range of uses and applications in various fields due to its unique features and capabilities. Some common applications of UWB technology include precision location and tracking systems [1,2], even in areas with poor GPS coverage. UWB technology is utilized in imaging and sensing [3]. It includes medical imaging, through-wall imaging, and ground-penetrating radar. UWB technology also finds applications in wireless communication for high-speed data transfer [4], enabling both short–range and long–range communication. Additionally, UWB technology is employed in automotive applications like collision avoidance, blind spot identification, and vehicle-to-vehicle communication. It is also used in security and surveillance applications to track intruders' movements in restricted areas and detect their presence [5].

Various optimization algorithms are commonly employed in the electromagnetic field to design antennas [6]. The most widely used

* Corresponding author.
E-mail addresses: islem.bouchachi@ensta.edu.dz (I. Bouchachi), reddaf.malek@gmail.com (A. Reddaf), mboudjerda@gmail.com (M. Boudjerda), k.hassoon@qu.edu.sa (K. Alhassoon), elect_babes@yahoo.fr (B. Babes), f.alsunaydih@qu.edu.sa (F.N. Alsunaydih), enas.ali1975@gmail.com (E. Ali), m.alsharef@tu.edu.sa (M. Alsharef), f.alsaleem@qu.edu.sa (F. Alsaleem).

https://doi.org/10.1016/j.heliyon.2024.e26337
Received 12 October 2023; Received in revised form 10 February 2024; Accepted 12 February 2024
Available online 21 February 2024

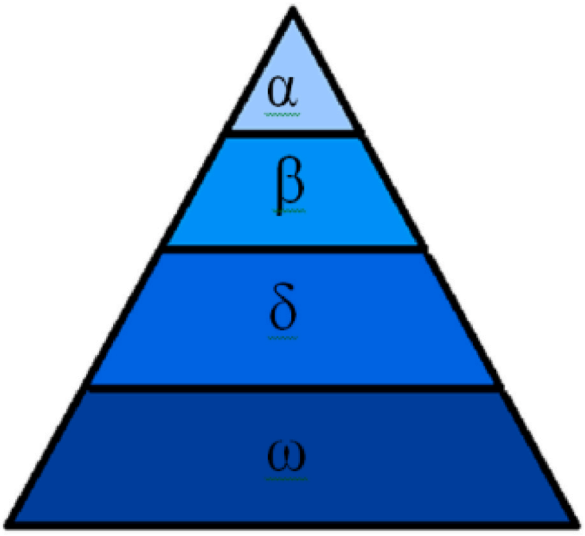

Fig. 1. Hierarchy of wolves.

algorithms are Genetic Algorithms (GA) [7], Particle Swarm Optimization (PSO) [8], Ant Colony Optimization (ACO) [9], Differential Evolution (DE) [10], and Grey Wolf Optimization (GWO) [11].

Grey Wolf Optimization is a population-based optimization algorithm that simulates the social hunting behavior of grey wolves. GWO requires minimal parameter tuning and can converge quickly to the global optimum. GWO was successfully utilized to improve UWB antenna arrays' beam-forming capabilities to produce high gain and guided radiation patterns [12]. It was applied for constructing UWB antenna matching networks to reduce reflection losses. The GWO was also employed to identify and classify different UWB antenna radiation patterns [13].

Split Ring Resonators (SRR) and Complementary Split Ring Resonator (CSRR) are artificially engineered materials that exhibit exotic electromagnetic properties, such as negative permittivity and negative permeability. They can be used to manipulate the propagation of electromagnetic waves.

They are often used in antenna design to enhance their performance [14]. SRR and CSRR can be implemented on the ground face of the antenna as a Defected Ground Structure (DGS), which creates band-stop or band-pass characteristics in the frequency response. They can also be implemented on the front face of the antenna as a slot [15].

In this work, we aimed to design a UWB antenna operating at [2.4 GHz–22 GHz] bandwidth and suitable not only for applications like WIMAX, WLAN, and ISM but also for short and long-range Millimeter-Wave Communications, including 5 G. We first started by designing a UWB antenna with a rectangular patch and partial ground plane, then we introduced a DGS on the ground plane and a disturbing pattern in the form of a slot on the patch. For this purpose, we developed an application programming interface (API) between HFSS and MATLAB, where GWO is utilized as an optimization method.

To enhance the robustness of our study, we fabricated the antenna and conducted a thorough comparison between the measured and simulated results. We have also provided a comparative table to assess the characteristics of our antenna in relation to those presented in similar research studies.

The novelty and technical contributions of the article include: (i) a conceptual development of a new optimized UWB antenna using the GWO approach, (ii) creation of a compact UWB antenna (47 × 35 mm) with good performance in terms of operational bandwidth (2.38–22.5 GHz) and high gain (9.34 dBi), (iii) comparison of the proposed antenna with the previously reported antennas in literature to show the uniqueness of this work in the form of a table. It is the first time that the DGS structure has been used in conjunction with GWO algorithm for UWB antenna design.

2. Grey wolf optimization (GWO) algorithm

GWO takes cues from the grey wolf packs' social structure and hunting habits. The tracking, surrounding, hunting, and attacking processes seen in grey wolf populations are mathematically simulated by the GWO program. Grey wolves participate in a three-stage hunting process that includes circling the prey, attacking the prey, and stratifying the social hierarchy [16].

Fig. 1 illustrates the social structure of grey wolves, highlighting the functions served by each hierarchy within the pack. However, GWO may have limitations in handling discrete or combinatorial optimization problems. It requires appropriate parameter tuning for optimal performance, and its convergence speed can be affected by problem complexity.

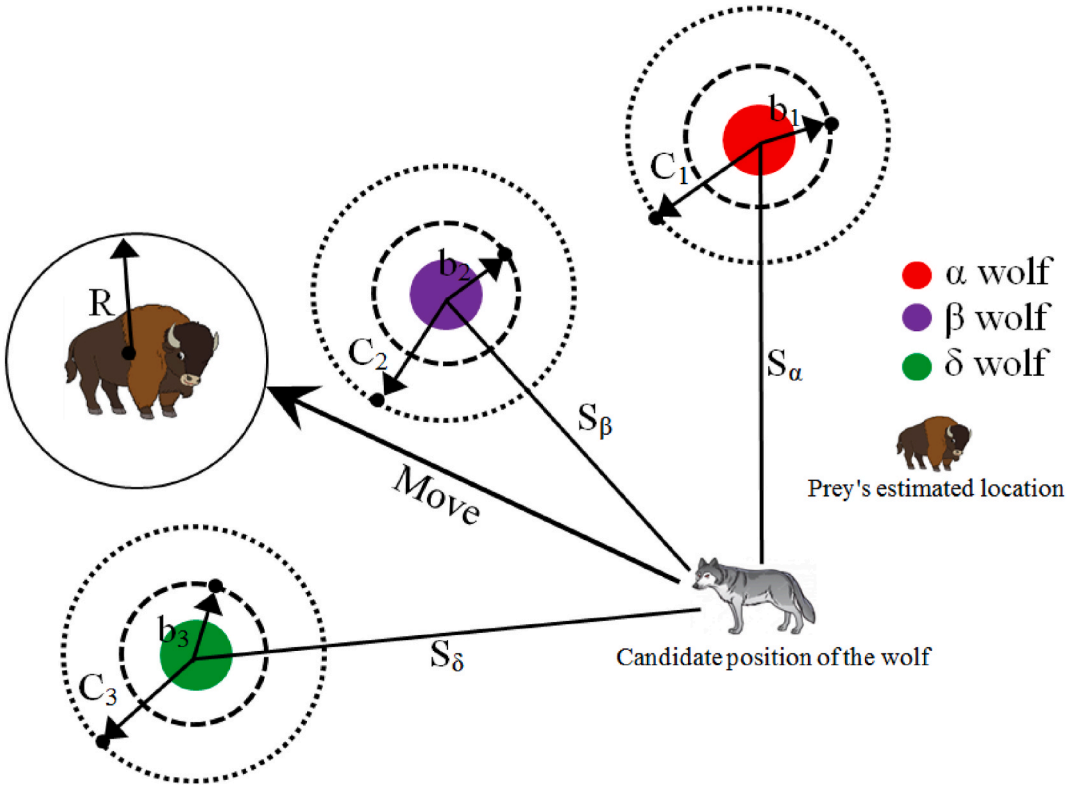

Fig. 2. Position updating in the GWO method.

2.1. Social hierarchy

Grey wolves can locate possible prey; this search is mostly carried out with the assistance of α, β, and δ wolves, as shown in Fig. 2. Each iteration retains the top three wolves (α, β, δ) in the current population, while the remaining individuals are designated as ω wolves.

2.2. Encircling the prey

Grey wolves encircle animals during hunting. The following equations (1)–(4) are used to quantify encircling behavior:

$$X(t+1) = X_p(t) - A.|C.X_P(t) - X(t)| \tag{1}$$

$$B = 2b.r_1 - b \tag{2}$$

$$C = 2.r_2 \tag{3}$$

$$b = 2 - 2(t/I) \tag{4}$$

where X represents the direction of the grey wolf, the prey's position vector is X_p; the most recent iteration is t; B and C are vectors of coefficients r_1 and r_2; r_1 and r_2 are random vectors in the range [0, 1]. The distance control parameter is denoted by b, its value decreases linearly from 2 to 0 throughout iterations. The maximum number of iterations is I.

2.3. Attacking the prey

During each cycle, the best three wolves (α, β, and δ) in the current population are retained, while the locations of other search are updated based on the position information of the three wolves. The agents position is given by the following equations (5)–(8):

$$X_1 = X_\alpha - B_1 \cdot |C_1 X_\alpha - X| \tag{5}$$

$$X_2 = X_\beta - B_2 \cdot |C_2 X_\beta - X| \tag{6}$$

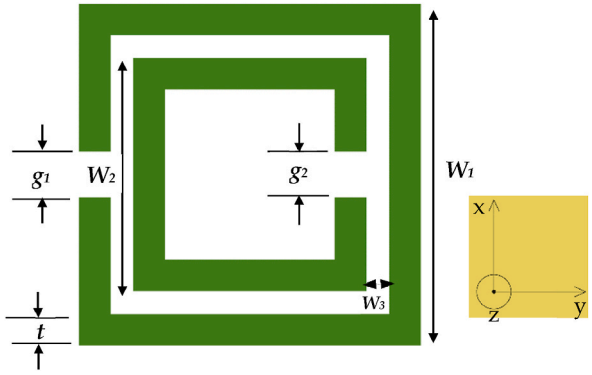

Fig. 3. SRR structure.

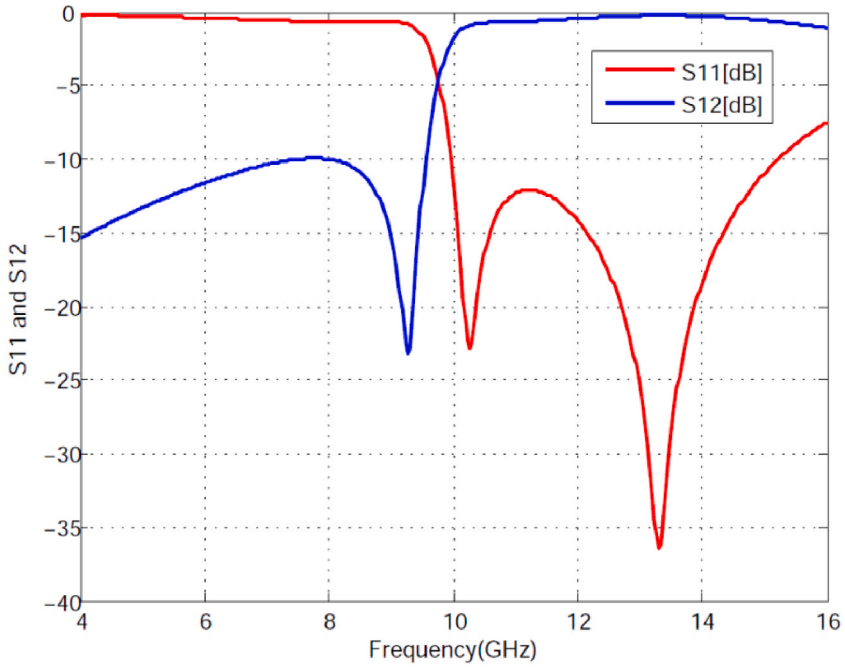

Fig. 4. S-parameters of simulation.

$$X_3 = X_\delta - B_3 \cdot |C_3 X_\delta - X| \tag{7}$$

$$X(t+1) = (X_1(t) + X_2(t) + X_3(t)) / 3 \tag{8}$$

in the following equations (9)–(11), X_α, X_β and X_δ are the position vectors of α, β and δ wolves, respectively. B_1, B_2, and B_3 are similar to B. C_1, C_2, and C_3 are similar to C.

$$S_\alpha = C_1 . X_\alpha - X \tag{9}$$

$$S_\beta = C_2 . X_\beta - X \tag{10}$$

$$S_\delta = C_3 . X_\delta - X \tag{11}$$

in equations (9)–(11) S_α, S_β, S_δ are the distances between the current candidate wolf and the top three wolves. The remaining contenders then randomly update their locations near the prey, guided by the current best three wolves. They begin searching for prey position information disorganizedly before focusing on assaulting the victim [17].

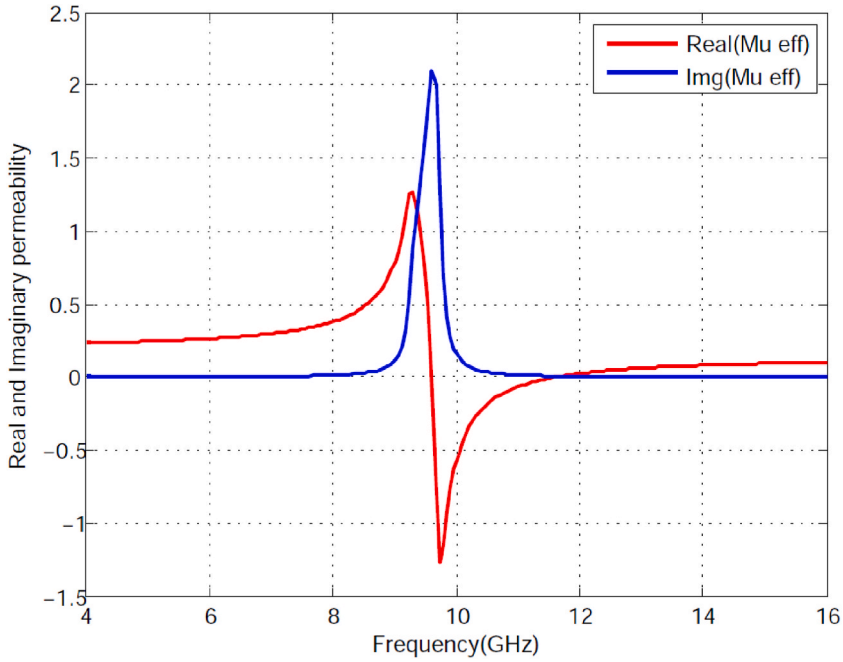

Fig. 5. Real and imaginary parts of SRR permeability.

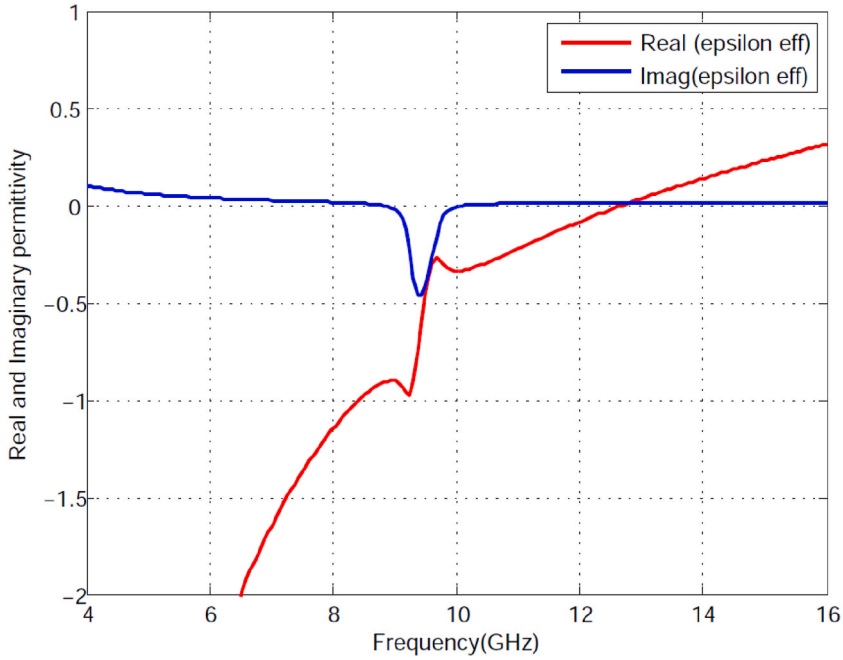

Fig. 6. Real and imaginary parts of SRR permeitivity.

3. Split ring resonator

In what follows, we will investigate the SRR shown in Fig. 3. Numerous researchers have extensively studied this type of resonator [18–20]. The SRR are composed of two rectangular loops with widths $w_1 = 2.2$ mm and $w_2 = 1.5$ mm as well as a split gap with widths $g_1 = g_2 = 0.3$ mm; added to the outer and inner rings, respectively, to allow capacitance effect to be introduced. The space between the inner and outer rings is $w_3 = 0.15$ mm and the width of the wire is $t = 0.14$ mm.

Altering the dimensions of the SRR not only affects the values of the equivalent circuit's RLC components but also enables the

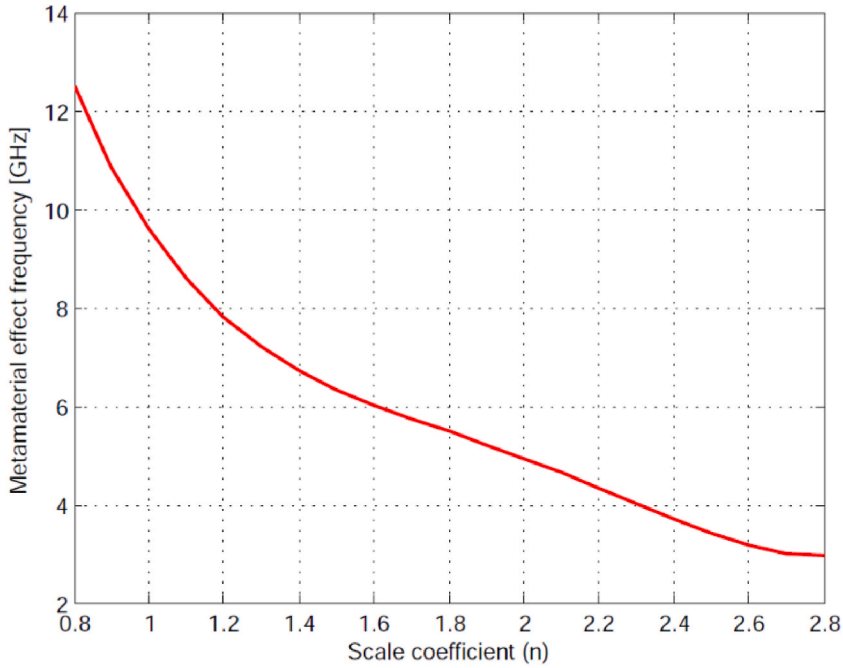

Fig. 7. Effect of SRR size variation on resonance frequency.

Fig. 8. CSRR structure.

material to exhibit metamaterial behavior at specific frequencies. This phenomenon is attributed to the emergence of negative permittivity and permeability [21,22].

The SRR properties are presented in terms of S-parameters; reflection coefficient (S_{11}) and transmission coefficient (S_{21}). An electromagnetic wave in the direction of the x-axis excites the structure to be tested, which is positioned between two waveguide ports. Perfect electric conductor (PEC) boundaries have been defined along the walls perpendicular to the *y*-axis, while perfect magnetic conductor (PMC) boundaries have been defined along the walls perpendicular to the z-axis. The obtained *S* parameters are shown in Fig. 4.

The Nicolson-Ross-Weir (NRW) technique [23,24] was utilized to acquire permittivity and permeability values from the Scattering parameters. The estimated real and imaginary parts of permittivity and permeability characteristics are presented in Figs. 5 and 6.

CSRR resonators are typically introduced to resonate at a frequency close to the operational frequency of the device. Given that our

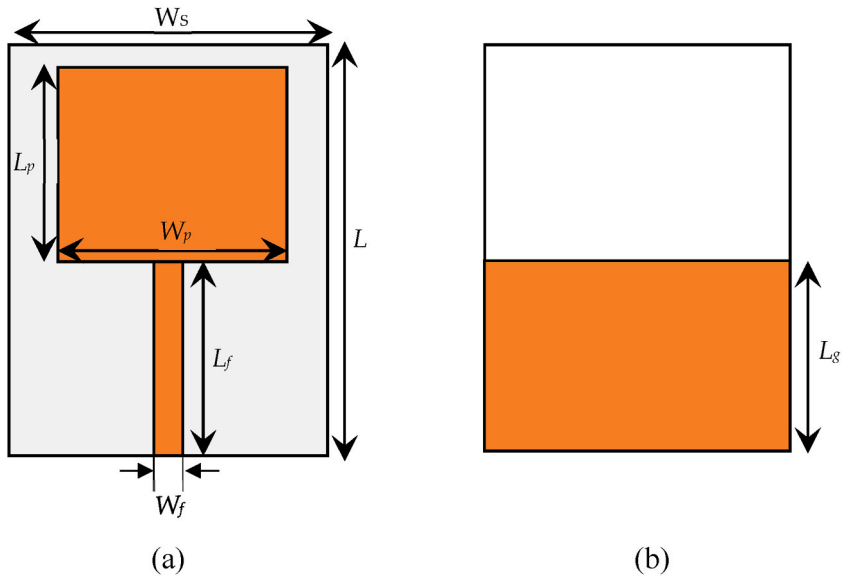

Fig. 9. UWB antenna design, (a) front view (Left), (b) back view (Right).

Table 1
Parameters of conventional antenna.

Patch	Dimensions (mm)
L	47
W	35
L_p	16
W_p	15
L_f	24
W_f	3
Lg	23

antenna operates in the UWB spectrum, a thorough study is essential to determine the optimal size for the resonator. To tackle this, we introduced a scaling coefficient, denoted as 'n' which will be multiplied by the dimensions of the initially studied resonator. This coefficient is integrated into the GWO program as an optimization variable. Fig. 7 illustrates how the resonance frequency varies with the scaling coefficient 'n' ranging from 0.8 to 2.8.

As observed in our study of the SRR, a parallel investigation was conducted for CSRR (Fig. 8), yielding remarkably similar outcomes. Both structures exhibit metamaterial behavior and resonate at the same frequency [25]. The most notable distinction lies in the fact that the SRR functions as an artificial magnetic material, whereas the CSRR operates as an artificial electric material.

4. Design of UWB antenna

For the design of our antenna, we preferred to proceed step by step to simplify the synthesis and to ensure a good convergence to the optimal solution. In the first step, we design a UWB antenna operating at [3.1 GHz, 10.6 GHz] bandwidth, using a rectangular patch and a partial ground plane [26]. For this purpose, we introduced five variables into the optimization algorithm: the dimensions of the patch (L_p and W_p), those of the feed line (L_f and W_f), and finally, the length of the partial ground plane (L_g) (see Fig. 9).

We chose FR-4 as a substrate for its cost-effectiveness and ease of use. The substrate has a dielectric constant of 4.4, a loss tangent of 0.02, and a thickness of 1.6 mm. In the second step, we introduced CSRRs on both sides of the antenna, and this step is detailed in the following section.

In the realm of optimization techniques, the evaluation function plays a crucial role as it distinguishes a good solution from a bad one. Our chosen evaluation approach is founded on two parameters: the reflection coefficient S_{11}, and the antenna's gain. This method imposes penalties on individuals who fail to meet the FCC standard criteria, which requires a reflection coefficient below −10 dB within the 3.1–10.6 GHz bandwidth. The remaining individuals are then ranked based on their gain performance. Consequently, the optimal individual boasts both a good bandwidth and a heightened gain. After executing the program, we derived the dimensions as presented in Table 1.

The obtained reflection coefficient S_{11} and the antenna gain are shown in Figs. 10 and 11.

The obtained antenna reaches a maximum gain value of 6.5 dB and a radiation efficiency of 92%.

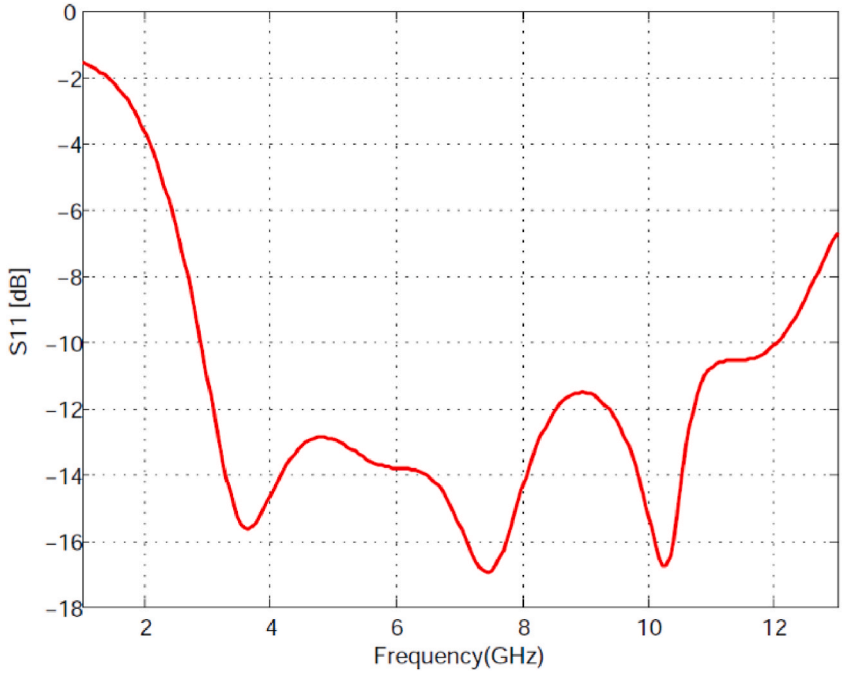

Fig. 10. Reflection coefficient of the initial UWB antenna.

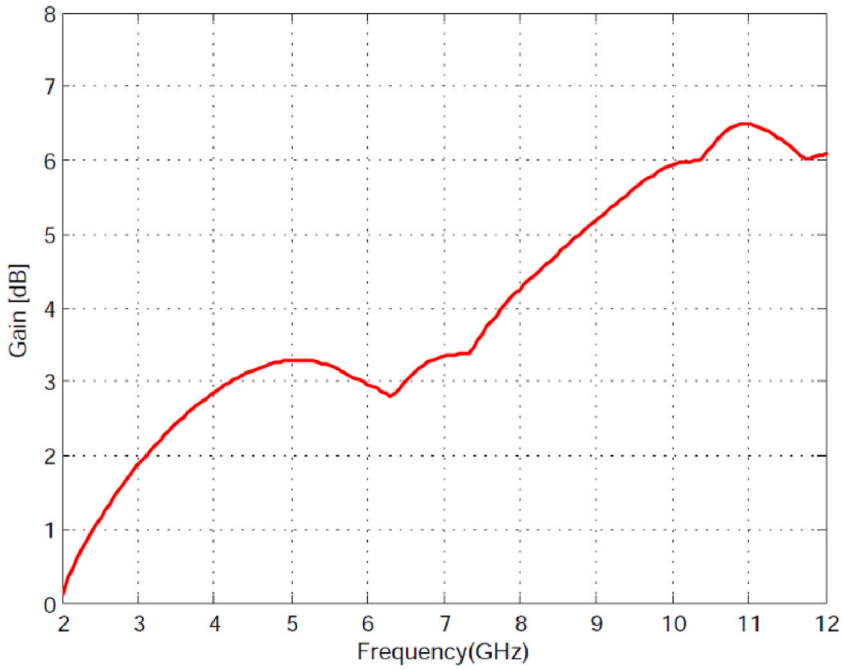

Fig. 11. UWB antenna gain.

5. Topology of our UWB antenna

The next stage is the design of the UWB patch antenna with the integration of CSRRs and using a similar numerical approach to the first (MATLAB, HFSS) API. We introduced six variables to the algorithm: the CSRRs position coordinates on both sides of the antenna (X_{slot}, Y_{slot}, X_{DGS} and Y_{DGS}) as shown on Fig. 12 and the CSRRs scaling coefficient n_1 and n_2. In our design, one resonator is added on the front face of the antenna (Patch face), and two resonators are placed symmetrically along the major median of the ground face.

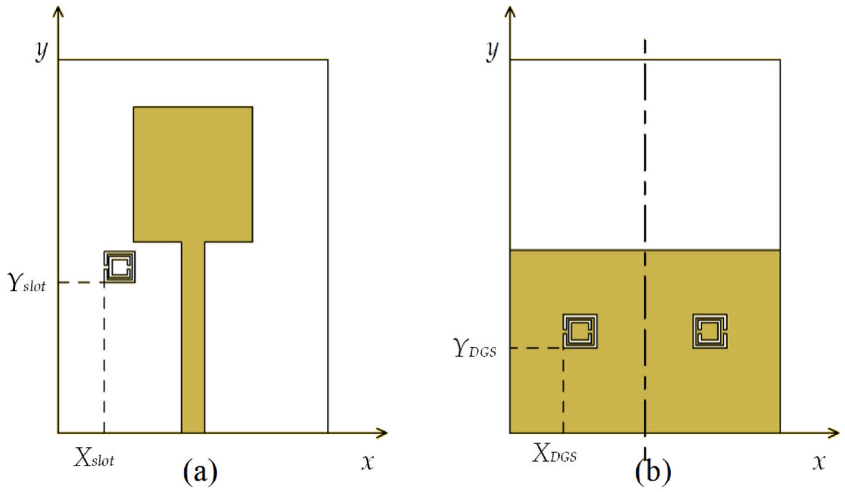

Fig. 12. Geometry of the proposed antenna: (a) front view (Left), (b) back view (Right).

Table 2
Parameters setting for GWO.

Parameters	Value
Search Agents	19
Dimension	6
Maximum iterations	200
Stopping criteria	10 stale generations

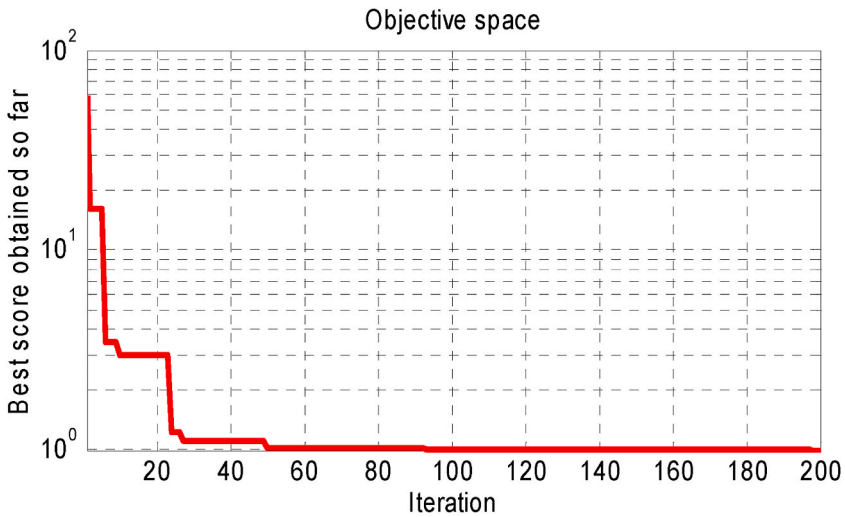

Fig. 13. Convergence curve of GWO algorithm.

Parameters such as population size and search space are among the factors that require tuning in the GWO algorithm to achieve optimal performance. Table 2 displays the algorithm's parameters, while Fig. 13 demonstrates its convergence. We used the same evaluation technique based on reflection coefficient and gain, but this time with [2.4 GHz–22 GHz] bandwidth penalization criteria. Once the optimization procedure is complete, the final design of the UWB antenna with CSRRs must undergo validation in terms of operating bandwidth, gain, efficiency, and radiation pattern.

6. Results and discussion

The optimized antenna is built using the photolithography technique to validate the resulting structure. Fig. 14 presents the final

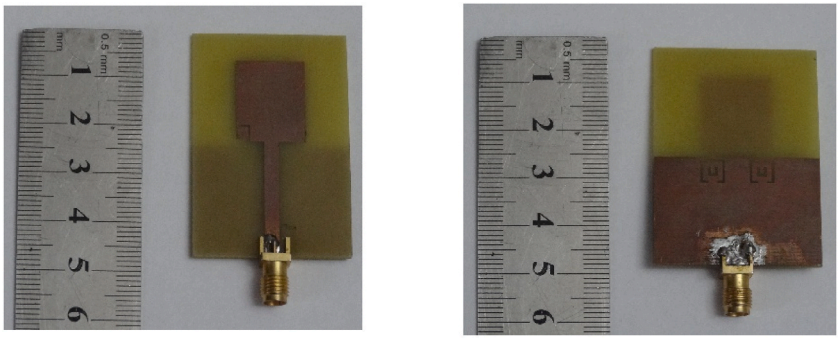

Fig. 14. Prototype of the proposed antenna: (a) front view (Left), (b) back view (Right).

Table 3
Optimized parameters of the antenna.

Slot position	1 Cell
Xslot	5.5 mm
Yslot n_1	20 mm
	2.2
DGS position	2 Cells
XDGS	10 mm
YDGS n_2	17.5 mm
	2.3

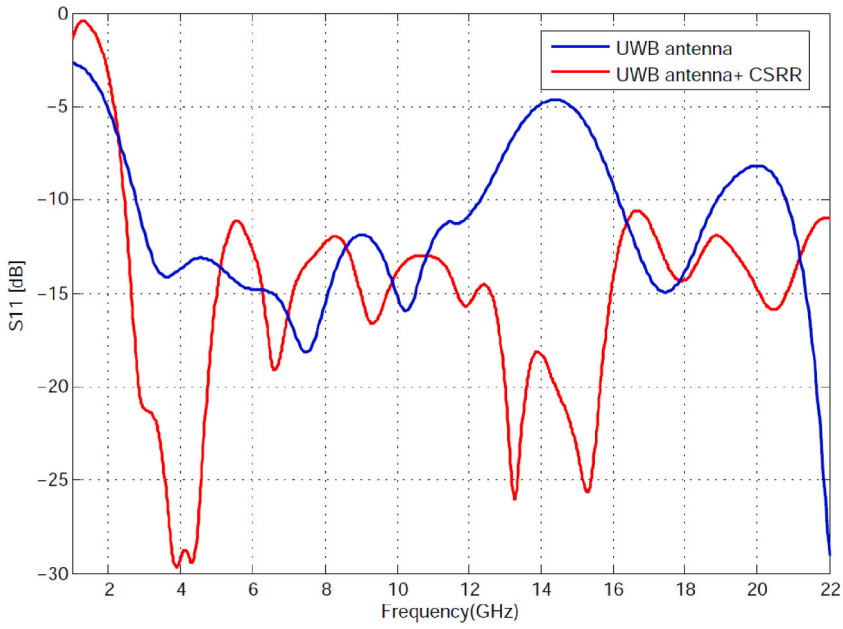

Fig. 15. Reflection coefficient before and after adding CSRR.

design, and Table 3 provides the antenna's optimized structural dimensions.

The simulated reflection coefficient S_{11} of the proposed antenna demonstrates a remarkable bandwidth coverage of 19 GHz, ranging from 2.38 GHz to 22 GHz, with a minimum return loss of −10 dB. Fig. 15 depicts the reflection coefficient before and after adding CSRRs. Whereas Fig. 16 shows a comparison of the simulated and measured reflection coefficient.

We plotted the antenna gain over the frequency range of 1–22 GHz, as shown in Fig. 17. The antenna exhibits an average gain of 5 dB, with a maximum value of 6.5 dB. Interestingly, this is nearly the same as the gain before introducing the CSRRs. However, a slight

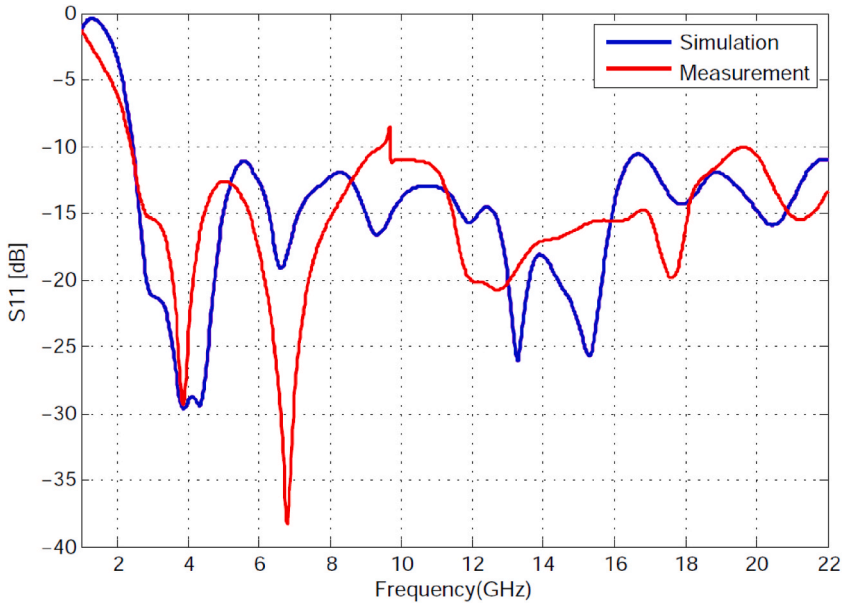

Fig. 16. Simulated and measured reflection coefficient of the proposed antenna.

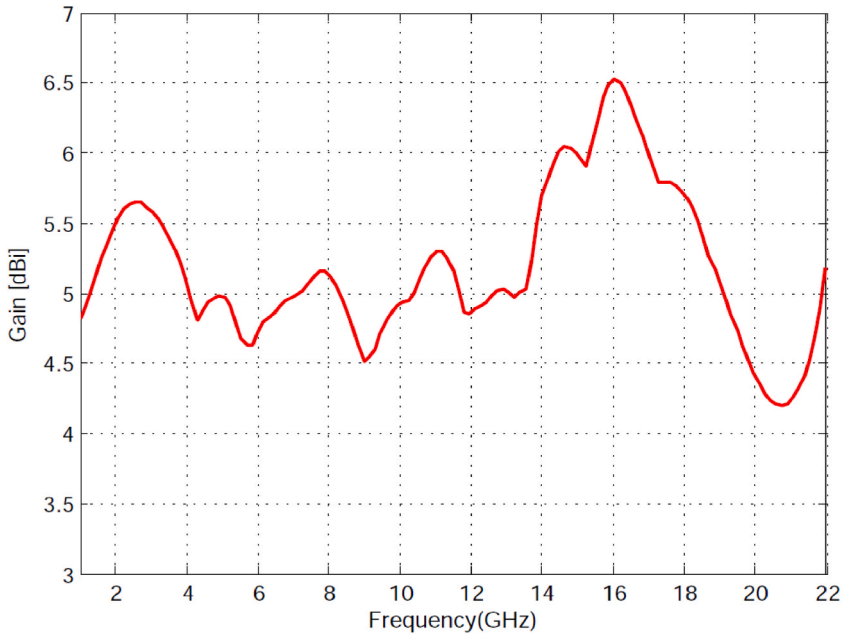

Fig. 17. CSSR antenna gain.

drop in radiation efficiency from 92% to 88% in the final antenna is worth noting.

Another crucial aspect in evaluating the effectiveness of a proposed antenna is the radiation pattern. Fig. 18(a–d) illustrates the simulated radiation pattern of the UWB antenna. The radiation pattern is observed in both the *xz* plane (*E*-plane) and the *xy* plane (*H*-plane) at resonant frequencies of 3, 6, 9 and 15 GHz.

Table 4 compares our antenna and several recently developed and proposed split ring resonator-based metamaterial and slot antennas in terms of different parameters (frequency, return loss, gain, bandwidth and dimensions). Notably, the suggested UWB antenna outperforms conventional antennas in terms of bandwidth and gain.

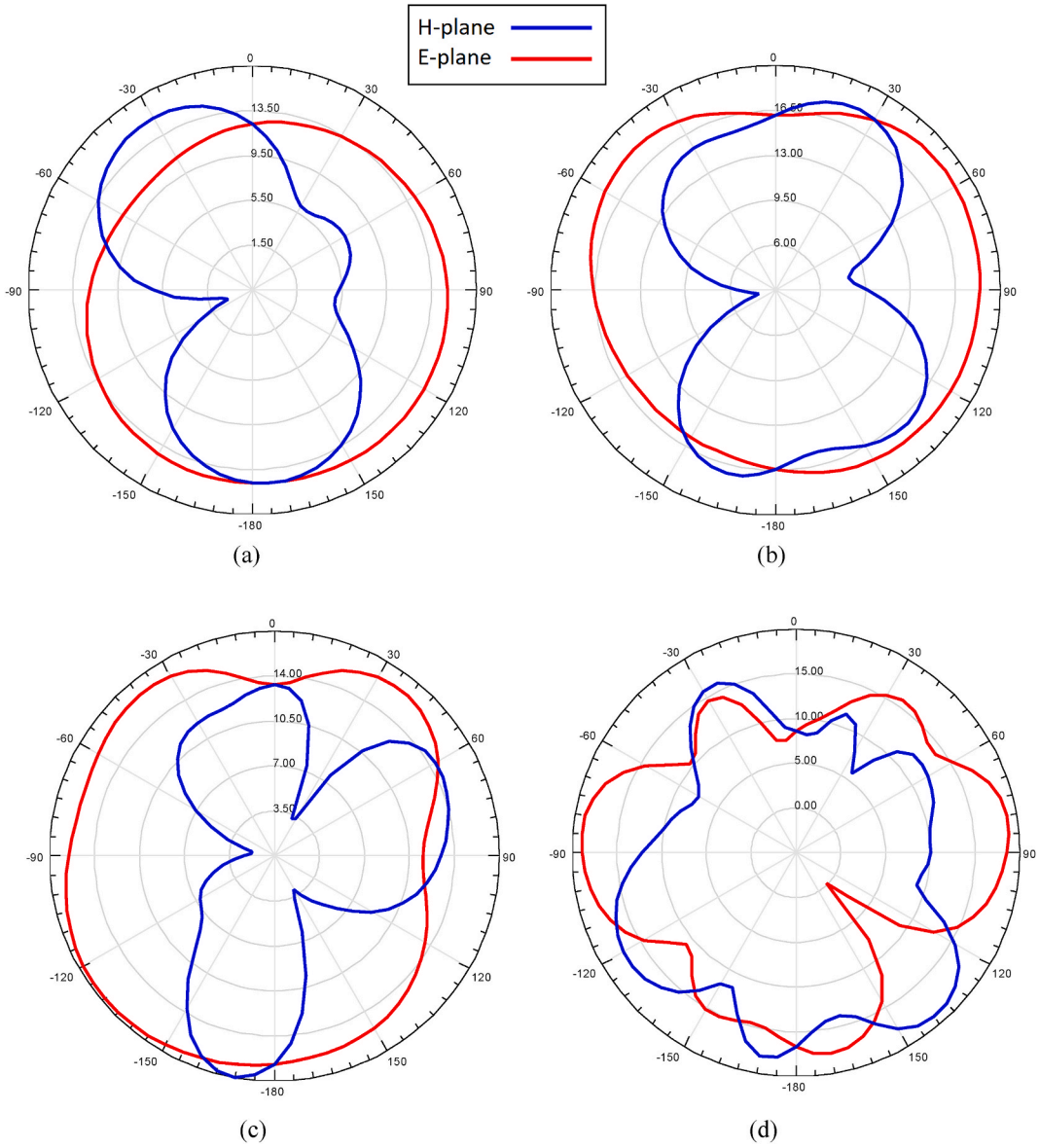

Fig. 18. Radiation patterns of the antenna at (a) 3 GHz, (b) 6 GHz, (c) 9 GHz, and (d) 15 GHz.

7. Conclusions

In this study, we proposed and investigated the design of a compact UWB antenna (47 × 35 mm) operating within the [2.38–22.5 GHz] bandwidth. This antenna is built upon the foundation of a conventional UWB antenna with a rectangular patch and partial ground plane, enhanced by incorporating CSRRs on both sides of the antenna, thus forming a DGS and slots on the patch. Introducing these resonators effectively doubled the antenna's bandwidth while maintaining stable and maximum gain across the entire frequency spectrum, ensuring good radiation efficiency. These attributes make this antenna suitable not only for standard UWB applications like WIMAX, WLAN, and ISM, but also for short- and long-range millimeter-wave communications, including emerging 5 G technology.

The effectiveness of the proposed design heavily depends on the chosen optimization algorithm, whereas the success of the optimization is contingent on algorithm parameters, convergence criteria, and initial parameters. The optimization process is based on a combined fitness function, primarily considering bandwidth and gain. While these factors are crucial, other considerations such as radiation pattern, antenna polarization, manufacturing feasibility and cost may not be explicitly addressed.

Table 4
Comparison of the proposed antenna with the conventional UWB antenna.

Antenna	*fr* (GHz)	Return loss (dB)	Bandwith (GHz)	Gain(dBi)	Dimensions (mm^2)
Kumar, G. Vijaya et al. [27]	2.45	–	2.58–12.24	–	50 × 44
	3.5	−27.03			
	5.15	−18.21			
	5.7	−13.52			
	7.5	−15			
Ullah, Shahid et al. [28]	2.45	–	3.09–40.2	5.9	35 × 35
	3.5	−22.5 dB			
	5.15	−13.32 dB			
	5.7	−15.03			
	7.5	−15			
Zhang, Ziyuan et al. [29]	2.45	–	2.5–10.6	–	33.6 × 43
	3.5	−22			
	5.15	−18.21			
	5.7	−9.53			
	7.5	−15			
Mahfuz, MM Hasan et al. [30]	2.45	–	2.9–10.7	5	45 × 34
	3.5	−22.03			
	5.15	−11.37			
	5.7	−11.42			
	7.5	−22			
Khedrouche et al. [31]	2.45	–	2.9–13.5	6.53	17 × 23
	3.5	−22.5			
	5.15	−25.22			
	5.7 GHz	−22.5			
	7.5 GHz	−13			
Proposed antenna	2.45	−11.42	2.38–22.5	6.5	47 × 35
	3.5	−19.23			
	5.15	−12.73			
	5.7	−15.02			
	7.5	−18.75			

Data availability

No data were used for the research described in this paper.

Funding & acknowledgments

Researchers would like to thank the Deanship of Scientific Research, Qassim University, for funding the publication of this project.

CRediT authorship contribution statement

Islem Bouchachi: Writing – original draft, Methodology, Investigation, Formal analysis. **Abdelmalek Reddaf:** Writing – original draft, Resources. **Mounir Boudjerda:** Writing – original draft, Software, Methodology, Investigation. **Khaled Alhassoon:** Supervision, Project administration, Funding acquisition. **Badreddine Babes:** Writing – original draft, Formal analysis. **Fahad N. Alsunaydih:** Supervision, Project administration, Funding acquisition. **Enas Ali:** Writing – review & editing, Supervision. **Mohammad Alsharef:** Writing – review & editing, Validation, Supervision, Project administration. **Fahd Alsaleem:** Supervision, Project administration, Funding acquisition.

Declaration of competing interest

The authors declare that they have no known competing financial interests or personal relationships that could have appeared to influence the work reported in this paper.

References

[1] T. Saeidi, I. Ismail, W.P. Wen, A.R.H. Alhawari, A. Mohammadi, Ultra-wideband antennas for wireless communication applications, Int. J. Antenn. Propag. (2019) 1–25, https://doi.org/10.1155/2019/7918765.
[2] P. Kumar, M.M.M. Pai, T. Ali, Ultrawideband antenna in wireless communication: a review and current state of the art, Telecommun. Radio Eng. 79 (2020) 929–942.
[3] A. Hossain, M.T. Islam, A.F. Almutairi, M.S.J. Singh, K. Mat, Md Samsuzzaman, An octagonal ring-shaped parasitic resonator based compact ultrawideband antenna for microwave imaging applications, Sensors 20 (2020) 1354.
[4] M. Rahman, M. NagshvarianJahromi, S. Mirjavadi, A. Hamouda, Compact UWB band-notched antenna with integrated bluetooth for personal wireless communication and UWB applications, Electronics 8 (2019) 158.

[5] Bocus MJ, Piechocki RJ. Passive unsupervised localization and tracking using a multi-static UWB radar network. In2021 IEEE Global Communications Conference (GLOBECOM) 2021 Dec 7 (pp. 01-06). IEEE.
[6] H. Bouchekara, Solution of the optimal power flow problem considering security constraints using an improved chaotic electromagnetic field optimization algorithm, Neural Comput. Appl. 32 (2019) 2683–2703.
[7] A. Reddaf, K. Ferroudji, M. Boudjerda, K.H. Cherif, I. Bouchachi, F. Djerfaf, Modeling of electromagnetic behavior of composite thin layers using genetic algorithm, 2017 5th International Conference on Electrical Engineering - Boumerdes (ICEE-B). IEEE (Oct. 2017), https://doi.org/10.1109/icee-b.2017.8192190.
[8] Y.-L. Li, W. Shao, L. You, B.-Z. Wang, An improved PSO algorithm and its application to UWB antenna design, IEEE Antenn. Wireless Propag. Lett. 12 (2013) 1236–1239.
[9] LV Tung, LH Manh, CD Ngoc, M Beccaria, P Pirinoli, Automated design of microstrip patch antenna using ant colony optimization, in: International Conference on Electromagnetics in Advanced Applications (ICEAA), IEEE, 2019, pp. 587–590.
[10] A. Belen, F. Güneş, P. Mahouti, Design optimization of a dual-band microstrip SIW antenna using differential evolutionary algorithm for X and K-band radar applications, ACES Journal 35 (2020) 778–783.
[11] S. Mirjalili, S. M. Mirjalili, and A. Lewis, Grey wolf optimizer, Adv. Eng. Software 69 (201) 46–61..
[12] M. Ghalambaz, R. Jalilzadeh Yengejeh, A.H. Davami, Building energy optimization using grey wolf optimizer (GWO), Case Stud. Therm. Eng. 27 (2021) 101250.
[13] K.N. Rao, V. Meshram, H.N. Suresh, Optimization assisted antipodal vivaldi antenna for UWB communication: optimal parameter tuning by improved grey wolf algorithm, Wireless Pers. Commun. 118 (2021) 2983–3005.
[14] Md Mushfiqur Rahman, Md Shabiul Islam, M. Tariqul Islam, S. Salem Al-Bawri, W. Hin Yong, Metamaterial-based compact antenna with defected ground structure for 5G and beyond, Comput. Mater. Continua (CMC) 71 (2022) 2383–2399.
[15] Y. Li, C.-Y.-D. Sim, Y. Luo, G. Yang, High-isolation 3.5 GHz eight-antenna MIMO array using balanced open-slot antenna element for 5G smartphones, IEEE Trans. Antenn. Propag. 67 (2019) 3820–3830.
[16] X. Yu, L. Huang, Y. Liu, K. Zhang, P. Li, Y. Li, WSN node location based on beetle antennae search to improve the gray wolf algorithm, Wireless Network 28 (2022) 539–549.
[17] B. Nayak, A. Mohapatra, K.B. Mohanty, Parameter estimation of single diode PV module based on GWO algorithm, Renewable Energy Focus 30 (2019) 1–12.
[18] D.R. Smith, D.C. Vier, Th Koschny, C.M. Soukoulis, Electromagnetic parameter retrieval from inhomogeneous metamaterials, Phys. Rev. 71 (2005), https://doi.org/10.1103/physreve.71.036617.
[19] A.B. Numan, M.S. Sharawi, Extraction of material parameters for metamaterials using a full-wave simulator [Education Column], IEEE Antenn. Propag. Mag. 55 (2013) 202–211.
[20] A. Reddaf, F. Djerfaf, K. Ferroudji, M. Boudjerda, K. Hamdi-Chérif, I. Bouchachi, Design of dual-band antenna using an optimized complementary split ring resonator, Appl. Phys. A 125 (2019), https://doi.org/10.1007/s00339-019-2483-2.
[21] K. Jairath, N. Singh, V. Jagota, M. Shabaz, Compact ultrawide band metamaterial-inspired split ring resonator structure loaded band notched antenna, Math. Probl Eng. 2021 (2021) 1–12.
[22] M. Boudjerda, et al., Design and optimization of miniaturized microstrip patch antennas using a genetic algorithm, Electronics 11 (2022) 2123, https://doi.org/10.3390/electronics11142123.
[23] A.M. Nicolson, G.F. Ross, Measurement of the intrinsic properties of materials by time-domain techniques, IEEE Trans. Instrum. Meas. 19 (1970) 377–382.
[24] M.S. Sharawi, M.U. Khan, A.B. Numan, D.N. Aloi, A CSRR loaded MIMO antenna system for ism band operation, IEEE Trans. Antenn. Propag. 61 (2013) 4265–4274.
[25] M.M. Bait-Suwailam, Electromagnetic field interaction with metamaterials, electromagnetic fields and waves, IntechOpen (May 15, 2019), https://doi.org/10.5772/intechopen.84170.
[26] R. Cicchetti, E. Miozzi, O. Testa, Wideband and UWB antennas for wireless applications: a comprehensive review, International Journal of Antennas and Propagation 2017 (2017) 1–45.
[27] GV Kumar, I Reddy, JS Satyanarayana, VS Vivek, DGS Based Ultra Wideband Antenna For Wireless Applications, InInternational Conference of Advance Research & Innovation (ICARI) (2020).
[28] S. Ullah, C. Ruan, M.S. Sadiq, T.U. Haq, A.K. Fahad, W. He, Super wide band, defected ground structure (DGS), and stepped meander line antenna for WLAN/ISM/WiMAX/UWB and other wireless communication applications, Sensors 20 (2020) 1735.
[29] Z. Zhang, S. Yang, M. Liu, S. Deng, L. Li, Design of an UWB microstrip antenna with DGS based on genetic algorithm, 2019 21st International Conference on Advanced Communication Technology (ICACT). IEEE (Feb. 2019), https://doi.org/10.23919/icact.2019.8701944.
[30] MM Hasan Mahfuz, et al., Design of UWB microstrip patch antenna with variable band notched characteristics, TELKOMNIKA (Telecommunication Computing Electronics and Control) 19 (2) (2021) 357–363.
[31] D. Khedrouche, T. Bougoutaia, A. Hocini, Design and analysis of miniaturized microstrip patch antenna with metamaterials based on modified split-ring resonator for UWB applications, Frequenz 70 (2016) 11–12.